Multiplexed Memory-Insensitive Quantum Repeaters

O. A. Collins, S. D. Jenkins, A. Kuzmich, and T. A. B. Kennedy
School of Physics, Georgia Institute of Technology, Atlanta, Georgia 30332-0430
(Dated: October 6, 2006)

Long-distance quantum communication via distant pairs of entangled quantum bits (qubits) is the first step towards technologies such as perfectly secure message transmission and distributed quantum computing. To date, the most promising proposals require quantum repeaters to mitigate the exponential decrease in communication rate due to optical fiber losses. However, quantum repeaters are exquisitely sensitive to the lifetimes of the memory elements they use. We propose a new approach based on a real-time hardware reconfiguration of multiplexed quantum nodes. This scheme should enable the construction of multiplexed quantum repeater networks that are largely insensitive to the coherence times of the quantum memory elements.

PACS numbers: 42.50.Dv,03.65.Ud,03.67.Mn

Quantum communication, networking, and computation schemes utilize entanglement between several elements as their essential resource. This entanglement enables phenomena such as quantum teleportation and perfectly secure quantum communication [1, 2, 3, 4, 5]. It is the generation of the entangled states, and the distance over which we may physically separate them, that determines the maximum range of quantum communication devices. To overcome the exponential decay in signal fidelity over the communication length, Briegel *et al.* [6, 7] proposed an architecture for noise-tolerant quantum repeaters, using an entanglement connection and purification scheme to extend the overall entanglement length using several pairs of quantum memory elements, each previously entangled over a shorter fundamental segment length. A promising implementation utilizing atomic ensembles, optical fibers and single photon detectors was proposed by Duan, Lukin, Cirac, and Zoller (DLCZ) [8].

The difficulty in implementing a practical quantum repeater is connected to short atomic memory coherence times and large loss rates in the transmission channels. Recently, advances in both atomic memories [9, 10, 11, 12] and in the generation of atomic memory-compatible photons which propagate in the low-loss optical fiber window [13] have been made. However, constructing quantum memory elements for the telecommunication window with the coherence times necessary for intra-continental communication remains challenging.

In this Letter we propose a new entanglement generation and connection architecture using a real-time reconfiguration of multiplexed quantum nodes. This strategy improves communication rates dramatically for short memory times. We propose an implementation of this scheme using atomic ensembles-based memory elements.

Entanglement-length doubling with ideal memory elements.— A generic quantum repeater consisting of $2^N + 1$ distinct nodes is shown in Fig. 1a. The first step is to generate entanglement between adjacent memory elements in successive nodes. We assume each such process succeeds with probability P_0. After entanglement generation one employs an entanglement connection process that extends the entanglement lengths from L_0 to $2L_0$, using either a parallelized (Fig. 1b), or multiplexed (Fig. 1c) architecture. This first entanglement connection succeeds with probability P_1, followed by subsequent entanglement-length doublings with probabilities P_2,...,P_N, until the terminal quantum memory elements, separated by $L = 2^N L_0$, are entangled.

For the simplest case of entanglement-length doubling with a single memory element per site ($N = n = 1$), we calculate the average time to successful entanglement connection for both ideal (infinite) and finite quantum memory lifetimes. This basic process is fundamental to the operation of the more complex N-level quantum repeaters. In essence, an N-level quantum repeater can be considered as a single entanglement connection of two $(N-1)$-level systems.

We define a random variable Z to be the waiting time for an entanglement connection attempt, involving measurements on the two internal memory elements (from here on times are measured in units of L_0/c, where the speed of light c includes any material refractive index). The random variable $Y \equiv 1$ if entanglement connection succeeds and zero otherwise. The time for each entanglement generation attempt is taken to be unity, as is the time required for each entanglement connection attempt. The total time to the first success is the sum of the waiting time between connection attempts and the time spent in unsuccessful trials,

$$\begin{aligned} T \ &= (Z_1 + 1)Y_1 + (Z_1 + Z_2 + 2)(1 - Y_1)Y_2 + \\ &\quad (Z_1 + Z_2 + Z_3 + 3)(1 - Y_1)(1 - Y_2)Y_3 + ..., \quad (1) \end{aligned}$$

from which it follows that

$$\langle T \rangle = \frac{\langle Z \rangle + 1}{P_1}, \quad (2)$$

since Z and Y are independent random variables. In the infinite memory time limit, Z is simply the waiting time until entanglement is present in both segments, i.e., $Z = \max\{A, B\}$, where A and B are random variables

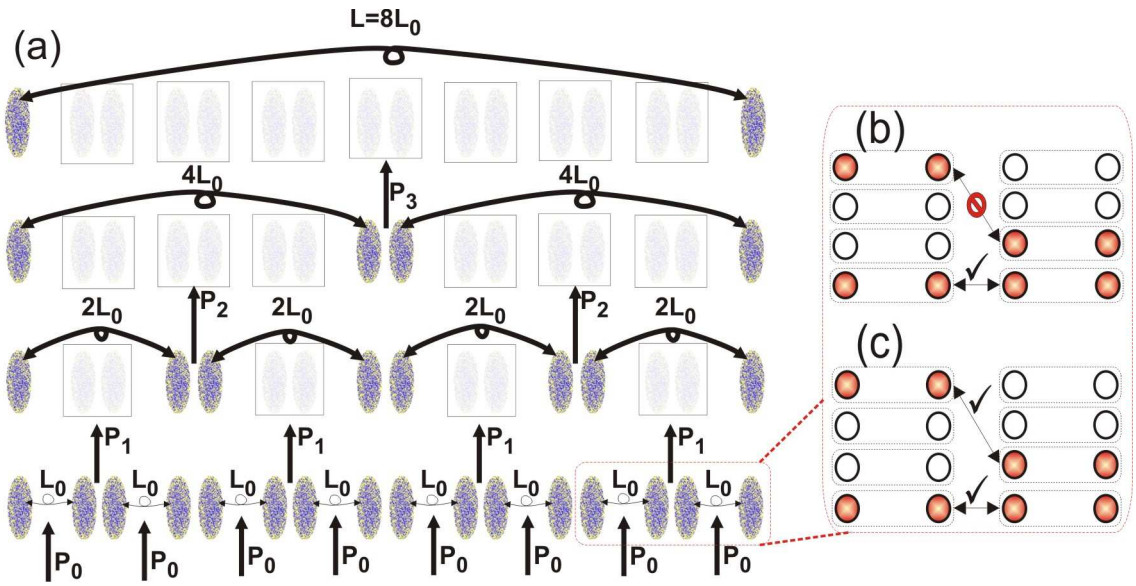

FIG. 1: (a) Successive entanglement connection processes of an $N = 3$ multiplexed quantum repeater which entangle quantum memory element nodes separated by a distance L. In addition to these two terminal nodes the network has seven internal nodes, each consisting of a pair of quantum memory sites. All sites contain n independent memory elements. Entanglement generation proceeds between elements in adjacent memory sites with probability P_0, creating entanglement in each segment of length L_0. In the lowest panel, shaded memory sites indicate eight successfully entangled segments. At the $N = 1$ level, entanglement connection between memory elements in alternate internal nodes proceeds with probability of success P_1, resulting in entanglement-length doubling and four entangled segments of length $2L_0$. The successfully connected nodes are shaded, while the nodes reset to their vacuum states are blank. The $N = 2$ and $N = 3$ levels produce similar entanglement connections with success probabilities P_2 and P_3, respectively. In each case these connections result in entanglement-length doubling operations, until success at the $N = 3$ level leaves the terminal nodes entangled, as shown in the upper-most panel. (b) and (c) show the topology of the n memory element sets within two adjacent segments. The parallel communication architecture,(b), connects entanglement only between memory elements with the same address. In contrast, multiplexing (c) uses a fast sequential scanning of all memory element addresses within a node to enable the connection of any available memory elements at the appropriate site.

representing the entanglement generation waiting times in the left and right segments. As each entanglement generation attempt is independent of previous attempts, A and B are both geometrically distributed with success probability P_0. Using the properties of the maximum of two geometrically distributed random variables, it follows that,

$$\langle T\rangle_\infty = \frac{3 - P_0^2}{P_0 P_1 (2 - P_0)}. \tag{3}$$

Entanglement-length doubling with finite memory elements.— For finite quantum memory elements Eqs. (1) and (2) still hold, but Z is no longer simply $\max\{A, B\}$. Rather it is the waiting time until the left and right segments are entangled within τ time units of each other, where τ is the quantum memory lifetime. For simplicity, we assume that the quantum memory acts as a step function. That is, entanglement is unaffected for τ, and destroyed thereafter. The variables A and B are defined as in the ideal case above. A new random variable $M \equiv 1$ if $|A - B| \leq \tau$, and zero otherwise. As A and B are geometrically distributed, Z is then given by,

$$\begin{aligned} Z &= \max\{A_1, B_1\} M_1 + (\min\{A_1, B_1\} + \tau \\ &+ \max\{A_2, B_2\})(1 - M_1) M_2 + ... \end{aligned} \tag{4}$$

From this and Eq. (2) it follows that

$$\langle T\rangle_\tau = \frac{\langle T\rangle_\infty - (\frac{1+P_0}{P_0 P_1}) \frac{q_0^{\tau+1}}{1-P_0/2}}{1 - \frac{q_0^{\tau+1}}{1-P_0/2}}, \tag{5}$$

where $q_0 \equiv 1 - P_0$. Since the entanglement generation probability suffers from transmission losses, P_0 is typically small compared to P_1. Fig. 2 illustrates the characteristically sharp increase in $\langle T\rangle_\tau$ for small τ. This suggests that more complex quantum repeaters will exhibit even poorer scaling, as N-level repeaters require many entanglement-length doubling successes.

Parallelization and Multiplexing.— Achievement of long coherence times remains an outstanding technical challenge. This motivates the exploration of approaches that might circumvent the poor scaling behavior at low memory times. One strategy is to engineer a system that

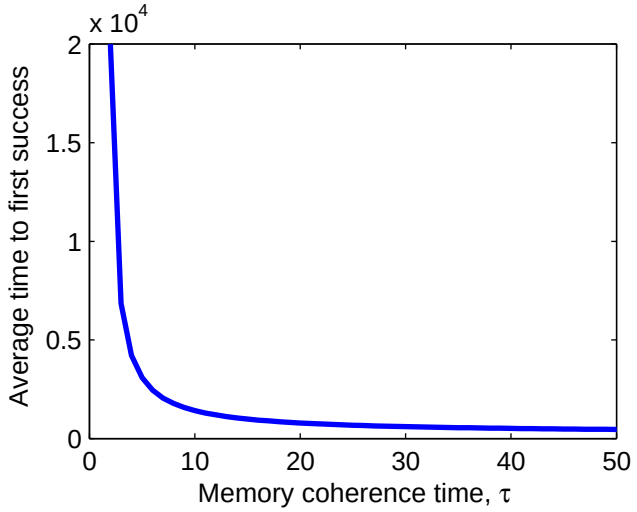

FIG. 2: Average success time as a function of quantum memory lifetime for an entanglement-length doubling process.Entanglement generation probability $P_0 = 0.01$, and entanglement connection probability $P_1 = 0.5$. Note that the minimum possible success time of 2, in units of light travel time, enforces a similar minimum of the quantum memory element lifetime.

compensates for low success rates by increasing the number of trials, placing $n > 1$ memory elements (element pairs) in each external (internal) node. This improves the chance of generating entanglement.

There are two basic ways to utilize this entanglement: parallelization and multiplexing. In the parallel scheme, the i^{th} memory element pair in one node interacts only with the i^{th} pair in other nodes, Fig.1b. Thus, a parallel quantum repeater with $n2^{N+1}$ total memory elements acts as n independent 2^{N+1}-element repeaters and connects entanglement n times faster.

A better approach is to dynamically reconfigure the connections between nodes, using information about entanglement successes to determine which nodes should be connected. In this multiplexed scheme, the increased number of node states that allow entanglement connection, compared to the parallel case, suggests an improved entanglement connection rate between the terminal nodes.

We now calculate the entanglement connection rate of an $N = 1$ multiplexed system. Unlike the parallel scheme, however, the entanglement connection rate is no longer simply related to the average time to the first success $\langle T\rangle_\tau$. Whenever one segment has more entangled element pairs than its partner, entanglement connection attempts do not reset the repeater to its vacuum state. Under this circumstance residual entanglement remains. Simultaneous successes and residual entanglement produce average times between successes smaller than $\langle T\rangle_\tau$. When residual entanglement is significantly more probable than simultaneous successes, we can approximate the resulting repeater rates. This is certainly the case in both the low memory time limit and whenever $nP_0 \ll 1$. Our approximation involves modifying the expression for the entanglement generation waiting time by including cases where the waiting time is zero due to residual entanglement. In Z of Eq. (4), the $\min\{A_j, B_j\}$ terms represent the waiting time to an entanglement generation success starting from the vacuum state. We modify $\min\{A_j, B_j\} \to \alpha \min\{A_j, B_j\}$, where 1-$\alpha$ is the probability of residual entanglement. With this change, Eq. (4) now produces the average time between successes. Using Eq. (2), the resulting rate is given by

$$\langle f\rangle_{\tau,n} = \frac{P_1(1-q_0^n)(1+q_0^n-2q_0^{n(\tau+1)})}{1+2q_0^n-q_0^{2n}-4q_0^{n(\tau+1)}+2q_0^{n(\tau+2)}+\alpha}, \tag{6}$$

where

$$\log\alpha \equiv \frac{2q_0^n(1-q_0^{n\tau}(2-q_0^n))}{1-q_0^{2n}}(n-1)\log q_0.$$

Fig. 3 compares the entanglement connection rates of the multiplexed ($\langle f\rangle_{\tau,n}$) and parallel ($n\langle f\rangle_{\tau,1}$) architectures for several different n values against a computer simulation of the multiplexed case. As expected, multiplexed entanglement connection rates do exceed those of the equivalent parallelized repeaters. The improvement from multiplexing in the infinite memory case is comparatively modest. However, the multiplexed connection rates are dramatically less sensitive to decreasing memory lifetimes when compared to parallelized systems. We note that for the given parameters the performance of the $n = 5$ multiplexed repeater exceeds that of its $n = 10$ parallelized counterpart, reflecting a fundamental difference in their dynamics and scaling behavior.

To further illustrate the memory insensitivity of multiplexed repeaters, we plot the fractional entanglement connection rate, relative to the infinite memory limit, for several values of n in Fig. 4. As parallelized rates scale by the factor n, such repeaters all follow the same curve, assuming identical system parameters. By contrast, multiplexed repeaters become less sensitive to coherence times as n increases. This improved performance in the low memory limit is a characteristic feature of the multiplexed architecture.

N-level quantum repeaters.— To calculate entanglement connection rates for $N > 1$ repeaters we proceed by direct computer simulation. It is our expectation that the qualitative behavior of the connection rates remains similar to the $N = 1$ case. Furthermore, the $N = 1$ analysis provides a check of the simulation results.

To simulate an N-level quantum repeater requires a specific choice of entanglement connection probabilities. We choose the particular physical implementation proposed by DLCZ [8]. For the DLCZ protocol, one must specify the total distance L, the number of segments 2^N,

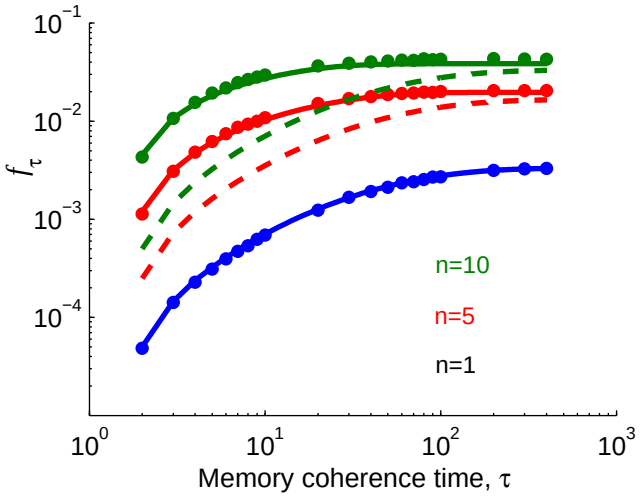

FIG. 3: Entanglement-length doubling rates for parallel and multiplexed architectures. Entanglement connection with an $N = 1$ quantum repeater, using $n = 1$, $n = 5$, and $n = 10$ elements per site and the same parameters as in Fig. 2. Solid lines represent multiplexed quantum repeaters, while dashed lines indicate parallelization. Data points denote simulated values for the multiplexed case. For lower memory lifetimes, the multiplexed $n = 5$ repeater outperforms the $n = 10$ parallel repeater.

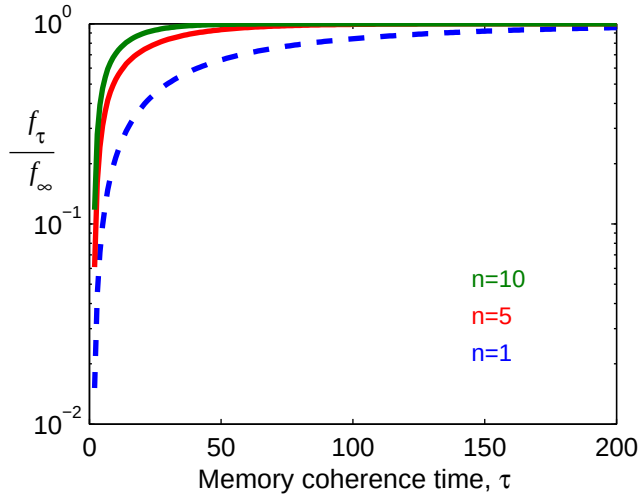

FIG. 4: Fractional entanglement-length doubling rates. Scaling behavior of multiplexed and parallel systems is compared for different values of n. All parallel architectures for arbitrary n follow the dotted line.

the loss γ of the fiber connection channels, and the efficiency η of retrieving and detecting an excitation created in the atomic ensemble based quantum memory elements.

The entanglement generation probability is given by $P_0 = \eta_0 \exp(-\gamma L_0/2)$, where η_0 is related to the fidelity $F \approx 1 - \eta_0$ [8]. A set of recursion relations gives the entanglement connection probabilities as a function of η: $P_i = (\eta/(c_{i-1}+1))(1-\eta/(2\beta(c_{i-1}+1)))$, $c_i \equiv 2c_{i-1}+1-\eta/\beta$, $i = 1, ...N$. Neglecting detector dark counts, $c_0 = 0$. Here $\beta = 1$ for photon number resolving detectors (PNRDs) [8] whereas $\beta = 2$ for non-photon resolving detectors (NPRDs). Though the two sets of recursion relations appear similar, there is an important physical difference: in the NPRD case, even ideal retrieval and detection efficiencies, $\eta = 1$, result in decreasing entanglement connection probabilities, $P_{i+1} < P_i$. In the PNRD case, ideal detectors result in constant connection probabilities, $P_{i+1} = P_i$. For values of $\eta < 1$ photon losses result in a vacuum component of the connected state in either case. For NPRDs, the inability to distinguish between one- and two-photon pulses leads to an additional vacuum contribution. Removing the vacuum component requires a final projective measurement, which succeeds with probability $\epsilon = 1/(c_3+1)$.

Consider a 1000 km communication link. Assume a fiber loss of $10\gamma/\ln 10 = 0.16$ dB/km, $\eta_0 = 0.05$, and a photonic retrieval and detection efficiency of $\eta = 0.5$. Taking $N = 3$ ($L_0 = 125$ km) results in the entanglement generation probability $P_0 = 0.005$. For concreteness, we treat the NPRD case. The above recursion relationships for NPRDs produce the entanglement connection probabilities: $P_1 = 0.4375$, $P_2 = 0.2655$, $P_3 = 0.1479$, and $\epsilon = 0.16$.

We begin by comparing the $N = 1$ analysis in Eqs. (3), (5), and (6) with simulated $N = 1$ results. Returning to Fig. 3 we observe that the simulation agrees well with both the exact predictions for $n = 1$, and the approximate predictions for $n > 1$. The slight discrepancies in the long memory time limit for larger n are quite uniform and are well understood from the influence of simultaneous connection successes, which were neglected in our analytic approximation. This produces predicted rates which, as expected, are slightly lower than the simulated results.

An N-level quantum repeater succeeds in entanglement distribution when it has entangled the terminal nodes with each other. Fig. 5 shows the entanglement distribution rate of a 1000 km $N = 3$ quantum repeater as a function of the quantum memory lifetime. We note the same characteristic memory insensitivity as in the multiplexed $N = 1$ repeater discussed earlier. Remarkably, for multiplexing with $n \gtrsim 10$ the entanglement distribution rate is essentially constant for coherence times over 100 ms. For memory lifetimes close or equal to the absolute minimum, set by the light-travel time between the terminal nodes, multiplexed repeaters with $n \gtrsim 10$ produce rates over a billion times faster than the equivalent parallel cases (not visible on the scale shown). We note that, for memory coherence times of less than 175 ms, one achieves higher entanglement distribution rates by multiplexing ten memory element pairs per segment than parallelizing 1000.

Communication and cryptography rates.— The DLCZ

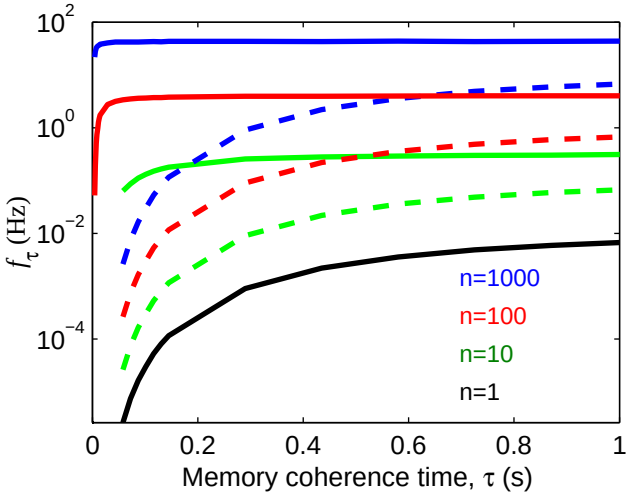

FIG. 5: Entanglement distribution over 1000 km. Simulated entanglement distribution rates for multiplexed (solid) and parallel (dashed) $N = 3$ quantum repeaters employing the DLCZ protocol with NPRDs for a range of n. The fiber loss, entanglement generation and connection probabilities are given in the text. Due to their larger simulation times, the $n = 1$ and parallel cases are simulated only for coherence times exceeding 60 ms. For coherence times longer than 100 msec, the entanglement distribution rate of multiplexed repeaters is almost flat for $n \gtrsim 10$. Over the same range, parallelized repeater rates decrease by two orders of magnitude. Note that in the low memory region the multiplexed $n = 10$ repeater outperforms an $n = 1000$ parallel quantum repeater.

protocol requires two separate entanglement distributions, within t_0, to communicate a single quantum bit, followed by two separate local measurements. Suppose the average success rate of entanglement distribution is f. The average probability of success within the requisite window t_0 is $p_s \simeq [1-(1-f)^{t_0}]^2$. The subsequent measurements involve the photonic retrieval and detection with efficiency η, and only half of the possible configuration states result in successful communication. This gives a communication rate of $R = \eta^2 p_s/2$. It is necessary that $t_0 < \tau$, as memory time is consumed during the entanglement distribution process. We have not considered the effects of dark counts, phase fluctuations, and other various sources of error. When these are non-negligible, standard linear-optics-based purification techniques [14, 15, 16, 17] could be applied to our multiplexing protocols.

Multiplexing with atomic ensembles.— A multiplexed quantum repeater could be implemented using cold atomic ensembles as the quantum memory elements. We propose to subdivide the cold atomic gas into n independent ensembles, each of which constitutes an individually addressable memory element, Fig. 1c. Dynamic addressing can be achieved by fast (sub-microsecond), two-dimensional scanning using acousto-optic modulators, which allow the coupling of each memory element to the same single-mode optical fiber. As an example, consider a cold atomic sample 400 μm in cross-section, confined in a three-dimensional far-detuned optical lattice. Assuming the addressing laser beams have waists of 20 μm, multiplexing $n > 100$ memory elements is feasible. To date, the longest single photon storage time is 30 μs, limited by Zeeman energy shifts of the unpolarized, unconfined atomic ensemble in the residual magnetic field [12]. By employing the magnetically-insensitive atomic clock transition in the optically confined sample, it will be possible to extend the storage time to tens of milliseconds. This should enable the implementation of multiplexed protocols, such as those proposed, sufficient for practical quantum communication over 1000 km.

Summary.— In conclusion, the proposed multiplexed repeater architecture greatly magnifies the impact of advances in quantum memory elements, translating each incremental advance in memory times into significant extensions in the range of quantum communication devices. The improved scaling outperforms massive parallelization with ideal detectors. These results are independent of the particulars of the entanglement generation and connection protocol. Ion-, atom-, and quantum dot-based systems should all benefit from multiplexing.

We are particularly grateful to T. P. Hill for advice on statistical methods, and we thank T. Chanelière and D. N. Matsukevich for helpful discussions. This work was supported by NSF, ONR, NASA, Alfred P. Sloan and Cullen-Peck Foundations.

[1] C. H. Bennett and G. Brassard, in *Proceedings of the International Conference on Computers, Systems and Signal Processing* 175 (IEEE, New York, 1984).
[2] C. H. Bennett *et al.*, Phys. Rev. Lett. **70**, 1895 (1993).
[3] A. K. Ekert, Phys. Rev. Lett. **67**, 661 (1991).
[4] D. Bouwmeester *et al.*, Nature (London) **390**, 575 (1997).
[5] E. Knill, R. Laflamme, and G. J. Milburn, Nature (London) **409**, 46 (2001).
[6] H. J. Briegel, W. Duer, J. I. Cirac, and P. Zoller, Phys. Rev. Lett. **81**, 5932 (1998).
[7] W. Duer, H. J. Briegel, J. I. Cirac, and P. Zoller, Phys. Rev. A **59**, 169(1999).
[8] L.-M. Duan, M. Lukin, J. I. Cirac, and P. Zoller, Nature (London) **414**, 413 (2001).
[9] D. N. Matsukevich and A. Kuzmich, Science **306**, 663 (2004).
[10] D. N. Matsukevich *et al.*, Phys. Rev. Lett. **95**, 040405 (2005).
[11] D. N. Matsukevich *et al.*, Phys. Rev. Lett. **96**, 030405 (2006).
[12] D. N. Matsukevich *et al.*, Phys. Rev. Lett. **97**, 013601 (2006).
[13] T. Chanelière *et al.*, Phys. Rev. Lett. **96**, 093604 (2006).
[14] C. H. Bennett *et al.*, Phys. Rev. Lett. **76**, 722 (1996).
[15] S. Bose, V. Vedral, and P. L. Knight, Phys. Rev. A **60**,

194 (1999).
[16] J.-W. Pan *et al.*, Nature (London) **410**, 1067 (2001).
[17] T. Yamamoto *et al.*, Nature (London) **423**, 343 (2003).